Advances in Automobile Engineering
ISSN: 2167-7670

Rajapakse et al., Adv Automob Eng 2015, 4:1
DOI: 10.4172/2167-7670.1000121

Research Article Open Access

Extremely Low-Cost Alternative for the Oxygen Reduction Catalyst of Fuel Cell

Rajapakse RMG[1,2]*, Senarathna KGC[1,2], Kondo A[3], Jayawardena PS[3] and Shimomura M[3]

[1]Department of Chemistry, University of Peradeniya, Sri Lanka
[2]Postgraduate Institute of Science, University of Peradeniya, Sri Lanka
[3]Graduate School of Science and Technology, Shizuoka University, Japan

Abstract

Fuel cells offer an enabling alternative energy technology for the present day useful energy crisis. However, one of the major obstacles of fuel cells in powering motor vehicles is the enormous cost associated with the catalysts used in both half-reactions which are Pt and Pt-Rh, respectively, for the anodic and cathodic half-reactions. Among several strategies put forward to reduce the cost of fuel cells, lowering of the amount of platinum used and replacing highly expensive platinum by low-cost catalysts are two major approaches to realize the development of fuel cell-powered motor vehicles. We have been pioneered in developing such low-cost catalysts for the difficult half-reaction, viz., the oxygen reduction half reaction of the fuel cells. We present here the development and the activity of Ag/Polypyrrole/Montmorillonite Clay catalyst which performs equally to expensive Pt-Rh catalyst used for the oxygen reduction half-reaction of fuel cells. We show that this catalyst functions very similar to highly expensive Pt-Rh catalyst and hence the former can be conveniently substituted for the latter in practical applications.

Keywords: Low-cost oxygen reduction catalyst; Polypyrrole; Montmorrilonite; Silver; Fuel cells

Introduction

Fuel cellis a devices capable of converting chemical energy change of a net chemical reaction, caused by the oxidation half reaction of a fuel that is taking place at the anode, and the reduction half reaction of oxygen that is taking place at the cathode, ($-\Delta G_{reaction}$), to electrical energy (nFE_{cell}). Heat may come as a by-product but the heat produced may also be harnessed to co-generate electricity. Fuel cells are clean energy sources which utilize the oxidation of a fuel such as hydrogen gas, methane gas, alcohols or any such fuel at the anode and the reduction of oxygen at the cathode. Although there are several different types of fuel cells, such as Phosphoric Acid Fuel Cell, Alkaline Fuel Cell, Molten Carbonate Fuel Cell, Direct Methanol Fuel Cell, Ceramic Fuel Cell and so on, the cathodic or reduction half reaction of all these fuel cells involve oxygen reduction. Oxygen for this purpose is obtained from air. Since the reactants of fuel cells at both electrodes are supplied externally, fuel cells produce very stable voltages, with time, since there is no depletion of reactants due to operation because they are continuously replenished by the external supply. Fuel cells resemble common Galvanic cells with the exception that the reactants are always supplied externally. Since the reactants are continuously replenished, fuel cells produce stable voltages over time. As such, fuel cells have become enabling energy technology for the world's energy portfolio. They offer clean energy more efficiently when compared to energy production by combusting gasoline and other fuels. Fuel cells, therefore, have the potential to replace the internal-combustion engine in vehicles and to provide power in stationary and portable power applications because they are energy-efficient, clean, and fuel-flexible. They are alternative power sources for remote stations and places where grid supply is not available. Honda Corporation has already debuted hydrogen fuel cell-powered FCV Concept at Detroit auto show [1], Toyota Mirai Fuel Cell Car will be in market by 2016 [2] and Mercedes Benz already produces F-Cell motor cars which are fuelled by hydrogen gas using a fuel pump [3].

The half-reactions taking place in $Pt/H_2(g)/acid/O_2(g)/Pt$ fuel cell are as follows.

$$\text{Anode } H_2(g) \rightarrow 2H^+(aq) + 2e^- \quad (1)$$

$$\text{Cathode } \tfrac{1}{2}\, O_2(g) + 2H^+(aq) + 2e^- \rightarrow 2H_2O \quad (2)$$

$$\text{Overall } H_2(g) + \tfrac{1}{2}\, O_2(g) \rightarrow H_2O \quad (3)$$

The maximum emf theoretically possible is + 1.229 V at 298 K. In general, the rates of electrochemical reactions can be conveniently monitored by measuring exchange current densities (J_o) and the $J_o$for the reaction (1) is around 1mA cm^{-2}, at 298 K, and is three orders of magnitude higher than that of reaction (2) [4,5]. The maximum obtainable emf is lowered by the over potentials required for each of the half reactions and is around 10 mV for the reaction (1) while it is over 400 mV for the oxygen reduction half-reaction(ORHR) (Reaction 2) at 0.4 mA cm^{-2} of usual operating current densities of the fuel cell. As such, oxygen reduction half reaction is considerably sluggish when compared to the hydrogen oxidation half reaction. It is, therefore, mandatory to have the best catalyst for the oxygen reduction half reaction and that is undoubtedly none other than platinum. The both the oxidation half reaction and the reduction half reaction of a fuel cell demand highly expensive catalysts such as Pt and Pt/Rh, respectively, making the cost of fuel cells prohibitively expensive. Researchers, over the past two decades, have done extensive research programmes to reduce the costs of these catalysts and the research has been carried out in four different strategies, viz., lowering the platinum group metal content by catalyst engineering particle morphology and crystal structure, alloying platinum with less expensive base metals such as Co, Mn, Ni and others, developing novel supports such as non-carbon

***Corresponding author:** Rajapakse RMG, Department of Chemistry, University of Peradeniya, Peradeniya 20400, Sri Lanka, Tel: +94-81-239-4442; E-mail: rmgr@pdn.ac.lk

Received July 22, 2015; **Accepted** August 06, 2015; **Published** August 10, 2015

Citation: Rajapakse RMG, Senarathna KGC, Kondo A, Jayawardena PS, Shimomura M (2015) Extremely Low-Cost Alternative for the Oxygen Reduction Catalyst of Fuel Cells. Adv Automob Eng 4: 121. doi:10.4172/2167-7670.1000121

supports and alternative carbon structures and researching non-platinum catalysts.

Obviously, the use of platinum black is not desirable, since, when platinum is used in its bulk form, the available surface area is very low and hence most of the interior platinum atoms are not utilized for their catalytic processes. One way to enhance the surface area of Pt particles is to decrease their size to a few nm diameter and to deposit them individually without particle aggregation on an inert support having large surface area such as highly porous carbon support. As such, the move from platinum black to catalysts made from carbon-supported-platinum has been researched due to significant cost reduction associated with this supported catalysiswhich is due to considerable lowering of the amount of platinum used. In the carbon-supported-platinum catalysts the platinum loading is typically 0.4 - 0.8 mg $cm^{-2}$and is a considerable reduction of amount of platinum used when compared to the use of platinum black as the catalyst with a platinum loading of 25 mg cm^{-2} [6]. The US Department of Energy (DOE) has set targets of 0.3 mg $cm^{-2}$of platinum loading for 2010 and 0.2 mg cm^{-2} for 2015. Nonetheless, these catalysts still rely on platinum.

Another way to reduce platinum content in the catalysts is to alloy it with other metals such as transition metals. Alloying with another metal not only reduces the amount of platinum usage but introduces many favourable effects such as enhancement of catalytic activity, selectivity and durability. Alloying platinum with transition metals, such as Mn, Fe, Ni, Co and Cu [5-16], has been shown to improve the rate of oxygen reduction half reaction when they are used as electro-catalysts for this half-reaction. It has been shown that improved catalytic activity is due to modified electronic structures of platinum by reducing the adsorption of unwanted species such as hydroxyl ions so as to make more active sites available for molecular oxygen adsorption. Use of alloy nanoparticles also adds further advantage of enhancing surface area of the electro-catalysts. It is also possible to tune the composition of the alloy composition in the nanoparticles by carefully selecting precursor concentrations and the synthesis temperature. For example, the use of 3:2 molar ratio of $Fe(CO)_5$ and $Pt(acaca)_2$ (where acac is acetlyacetone) gives $Pt_{0.52}Fe_{0.48}$, 2:1 gives $Pt_{0.48}Fe_{0.52}$ and 4:1 gives $Pt_{0.3}Fe_{0.7}$ alloy compositions [17]. Controlled synthesis of Pt_xNi_{1-x} nanoparticles can result in alloy compositions of Pt_3Ni, PtNi, $PtNi_2$ and $PtNi_3$ when 1:1.5, 1:2, 1.3.7 and 1:5 molar ratios of $Pt(acac)_2$ and $Ni(acac)_2$ are used [18,19]. Although alloying seems to solve the major problem of reducing platinum content in the electro-catalysts and may seem to improve performances, their long term stability has become a serious issue when these catalysts are used in reactive environments such as in acidic solutions used in fuel cells. Since most of these transition elements react with acids the leakage of their ions into the solution with time is an unavoidable problem inherent in these systems.

We have been pioneered in developing non-platinum catalysts for the oxygen reduction half reaction of fuel cells by developing extremely low-cost catalysts based on nano composites of montmorillinite clay (MMT), electronically conducting polymers such as polypyrrole (PPY) and the reduced form of the oxidising ion. We first published MMT/PPY/Ce(III) system as an efficient electro-catalyst for oxygen reduction [20] and the publication has been immediately reviewed in a book entitled "Chalcogens: Advances In Research And Application" [21]. We now have several similar systems such as Fe(II)/Polypyrrole/MMT, Ag/Polypyrrole/MMT, Pd/Polypyrrole and Polypyrrole/Porphyrine structures and metalated Porphyrine structures, all of which show promising results for oxygen reduction and stand as substantially low-cost alternatives to currently used Pt-Rh catalyst for the ORHR of fuel cells. As such, fuel cell power can be harnessed at reasonably low cost in the near future for the environmentally benign greener power production. Described in this manuscript is the low-cost Ag/Polypyrrole/MMT catalyst for the ORHR of fuel cells.

Experimental

Materials

All chemicals used were of analytical grade Sigma-Aldrich Chemicals. Silver(I) nitrate (Assay>99%, $AgNO_3$), nitric acid 68%, freshly distilled pyrrole, commercial Bentonite clay (montmorrilonite) and Nafion 5% w/w in propanol solution were used in this study.

Method

Bentonite (MMT) was purified by the procedure given below. 20 g of MMT clay was suspended 500 mL distilled deionized water by shaking for 12 at room temperature remove water soluble impurities. The dispersion was centrifuged and the supernatant discarded. The remaining solid was washed two more times by repeating the same procedure. The solid was then suspended in 1 M HNO_3 and the above procedure repeated. It was then suspended in 6% H_2O_2 and the procedure was repeated thrice. This has resulted in pure MMT with H^+ as the interlayer cations (MMT-H^+). 50 ml Ag^+ aqueous solution was prepared by dissolving $AgNO_3$ (0.429 g) in 10mM nitric acid solution (50 ml). Purified Bentonite clay (MMT) was dispersed by stirring for 24 h in the above solution. The suspension was then centrifuged and the supernatant discarded. The solid obtained was washed thoroughly with distilled water by repeating thrice the dispersion, centrifuging and supernatant discarding to obtain MMT-Ag (I). 1 g of MMT-Ag(I) was suspended in 0.1M HNO_3 (40 mL) by stirring and distilled pyrrole (175 ml) was then added dropwise and stirred for further 12 h. Then the solution was allowed to settle and a black coloured precipitate obtained was centrifuged and the clear supernatant was discarded. The composite solid obtained was washed with distilled water and acetone and allowed to dry in ambient laboratory conditions. It is termed Ag/PPY/MMT.

Characterization

The Ag/PPy/MMT composite was characterized by the Furrier transform infrared (FTIR) spectra which were recorded on a ShimadzuIRPrestige 21 instrument, using the standard KBr pellet method. X ray diffraction (XRD) studies were effected from a Siemens D5000 Powder X-ray Diffractometer, with the Cu K_α (wavelength= 0.1540562 nm) radiation, at the scan rate of $1^\circ min^{-1}$. X-ray fluorescence (XRF) studies were carried out using FisherXRF9400. XPS studies of the samples were done on Shimadzu, ESCA-3400.

To carry out the electrochemical studies the working electrode was prepared as follows. Ag/PPy/MMT (10 mg) was dispersed in ethanol (2 ml) and Nafion solution (10 ml) was then added. Then the mixture was soniccated for 10 min. The catalytic ink (10 ml) thus obtained was deposited on a cleaned and polished glassy carbon (GC) electrode. This electrode was used as the working electrode to run cyclic voltammogrammes(CVs) using MetrohmPotentiostat 101 and NOVA 1.7 software. Potentials were applied with respect to the saturated calomel electrode (SCE) and a Pt disk was used as the counter electrode. Scan rate used was 50 mVs^{-1} and 0.10 M KOH(aq) was used as the electrolyte solution. CVs were recorded in N_2-purged and O_2-saturated solutions.

Results and Discussion

Characterization of the samples prepared

Figure 1 shows X-Ray Diffractogrammes of (a) MMT-H^+ and (c) Ag/PPY/MMT recorded at room temperature as well as for all three samples heated for 2 h, at 150°C, prior to measurement. The major peaks appearing at 2θ=5.88, 5.66, 5.32, at room temperature for MMT-H^+ and MMT-Ag(I) and Ag/PPY/MMT, respectively. When heat-treated at 150°C, for 2 h to remove all hydration water these peaks shift to 9.72, 7.123 and 5.32, respectively. The d-spacings calculated from the major peaks for all these cases at both temperaturesare tabulated in Table 1.

It is evident from the date depicted in Table 1 that, at the room temperature, the d-spacing of MMT is strongly influenced by the hydration sphere of the interlayer cations, in this case H^+. When heat-treated at 150°C, for 2 h, all of the hydrated water molecules are removed and the presence of bare H^+cations within the interlayer spacing gives a d value of 9.72 Å, whereas the as prepared samples show a d-spacing of 15.01 Å. Since the thickness of a water monolayer around an ion is ~3 Å, it is evident that there are two waters aroundH^+ ions present within the interlayer spacings. The change of d-spacing due to the exchange for other cations such as Ag^+, is therefore, not possible to determine when these cations are surrounded by different numbers of water layers. However, direct comparison can be conveniently achieved if these water layers are removed. Therefore, the values of the d-spacings of samples heat-treated at 150°C correlate directly to the sizes of bare species in the absence of hydration spheres. As such, the replacement of H^+ ions by Ag^+ions is manifested by the increase in the d-spacing by 2.68 Å. Introduction of PPY to the interlayer spaces of PPY has further increased the d-spacings by 4.40 Å. It is interesting to note that the d-spacing of Ag/PPY/MMT has not changed due to heat treatment. This is because while Ag atoms do not get hydrated the presence of the conducting polymer PPY also results in the expelling of water from the interlayer spaces. As such, there isn't any hydrated water present within the interlayers in the composite Ag/PPY/MMT even at the room temperature. Thus the XRD data provides indirect evidence to the exchange of H^+ by Ag^+ and also the formation of PPY to the interlayer spaces when pyrrole is introduced. This so happens

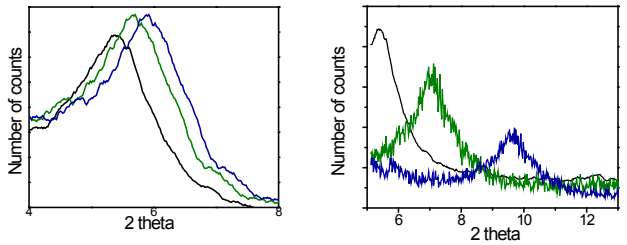

Figure 1: XRD spectrum of **(a)** MMT-H^+ **(b)** and MMT-Ag(I), **(c)** Ag/PPY/MMT composite recorded **(i)** at room temperature and **(ii)** at 200°C.

Composite	d-Spacing (A^0)	
	R.T.	150°C
MMT-H+	15.01	9.72
Ag(I)/MMT	15.6	12.4
Ag/PPY/MMT	16.6	16.6

Table 1: The d-spacings calculated for H^+-exchanged montmorillonite clay (MMT-H^+), Ag(I)-Exchanged MMT and Ag/Polypyrrole/Montmorillonite (Ag/PPY/MMT) nanocomposite at room temperature and for the same samples heat-treated at 150°C for 2 h prior to measurements.

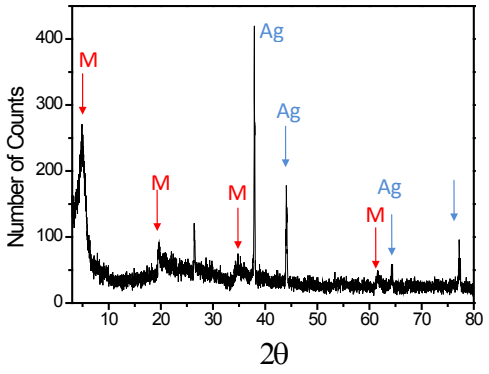

Figure 2: X-Ray Diffractogramme of the Ag/polypyrrole/montmorillonitenano composite in the full range.

MMT sample	Percentage Composition of Elements%			Atomic ratio
	Si	Fe	Ag	Si: Fe: Ag
H^+-MMT	69.69	22.45	0.00	3:1:0
Ag(I)/MMT	48.07	20.03	31.89	12:5:8
Ag /PPY/MMT	57.93	15.94	26.13	16:5:8

Table 2: Percentage composition of Si, Fe and Ag calculated from X-Ray Fluorescence for the H^+-montmorillonite, Ag(I)-exchanged MMT and Ag/PPY/MMT Nanocomposite.

by the oxidative polymerization of pyrrole by Ag^+cations thus forming PPY and Ag(0).

The presence of Ag(0) in Ag/PPY/MMT is verified by its XRD spectrum recorded in the full range of 2θ values from 0° to 80° which is shown in Figure 2. The corresponding diffraction peaks appearing at 2θ values of 5.32, 19.9, 35.0 an. 62.5 are assigned to diffraction pattern of MMT according to the card number while those appearing at 2θ values of 38.2, 44.3, 64.5 and 77.0 are assigned to be due to reflections from Basal planes of 111, 200, 220 and 311 respectively of Ag metal as JCPDS card Number 04-0783. This confirms the presence of both MMT and Ag(0) in the Ag/PPY/MMT composite. The PPY phase present within the interlayer spaces of MMT is amorphous and hence XRD peaks are not observed for PPY. X-ray fluorescence spectroscopy presents as a convenient tool to compare the atomic percentages of various elements present in the bulk sample though our XRF is capable only of detecting elements with atomic number higher than 13. As such, the percentages calculated are those from measured elements excluding the elements that are not able to measure. As such, the quantitative values may not be accurate though the ratios of elements present in the samples can be accurately obtained. Table 2 gives the percentages of Si, Fe and Ag calculated from XRF data. It is interesting to note that both Ag(I)/MMT and Ag/PPY/MMT samples contain appreciable amounts Ag and in equal amounts in the two samples as per Si to Ag atomic ratio. This is a direct evidence to prove the presence of Ag in both samples. When Na^+ ions in MMT are exchanged for Ag(I) ions, Ag(I)/MMT clay is formed. When pyrrole (Py) is introduced to Ag(I)/MMT, Ag(I) ions act as an oxidizer to Py to form $Py^{+\cdot}$ cation radicals to initiate the polymerization of Py. $Py^{+\cdot}$ then combine with Py molecule and form Py-Py^+ radicals and so on for propagating the polymerization reaction to eventually form PPY. Ag(I) ions are then reduced to Ag(0) thus resulting in the eventual product Ag/PPY/MMT. It is interesting to note that for each Ag(I) ion that was present originally there is one cation radical in the PPY chains for the conservation of the total charge.

FT-IR spectra of the three samples are depicted in Figure 3. The FT-IR band assignments are given in Table 3. All the characteristic bands of MMT and PPY are obtained as shown in Table 4 thus confirming the presence of PPY within the interlayers of MMT. Having shown that the composite Ag/PPY/MMT does contain all three components, namely, Ag, PPY and MMT, next strategy is to find out how these species are arranged in the composite. This study can be done by using a surface analytical technique such as X-Ray Photoelectron Spectroscopy of the samples. The XPS measures the surface composition of solids up to 2 nm depth from the surfaces of the solid. The XPS spectra of Ag/PPY/MMT are shown in Figure 4. The XPS spectra shows the presence of Si, Al, O originating from MMT, Ag from Ag and C and N from PPY. However, XPS spectrum of Fe is not seen though XRF has clearly identified the presence of Fe in this sample. It is possible that HNO_3

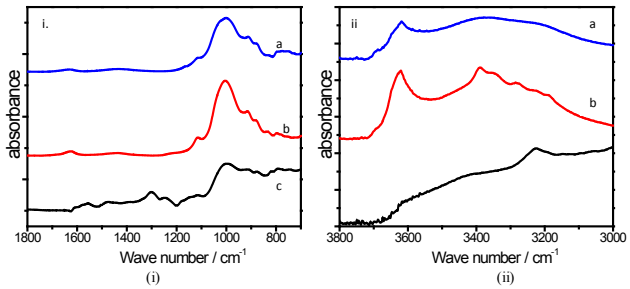

Figure 3: FTIR data for H^+-montmorrilonitea (MMT-H^+), b) MMT-Ag(I) and c) Ag/Polypyrrole/MMT composites in the wavenumber range from **(i)** 700 to 1800 cm^{-1} and **(ii)** 3000 to 3800 cm^{-1}.

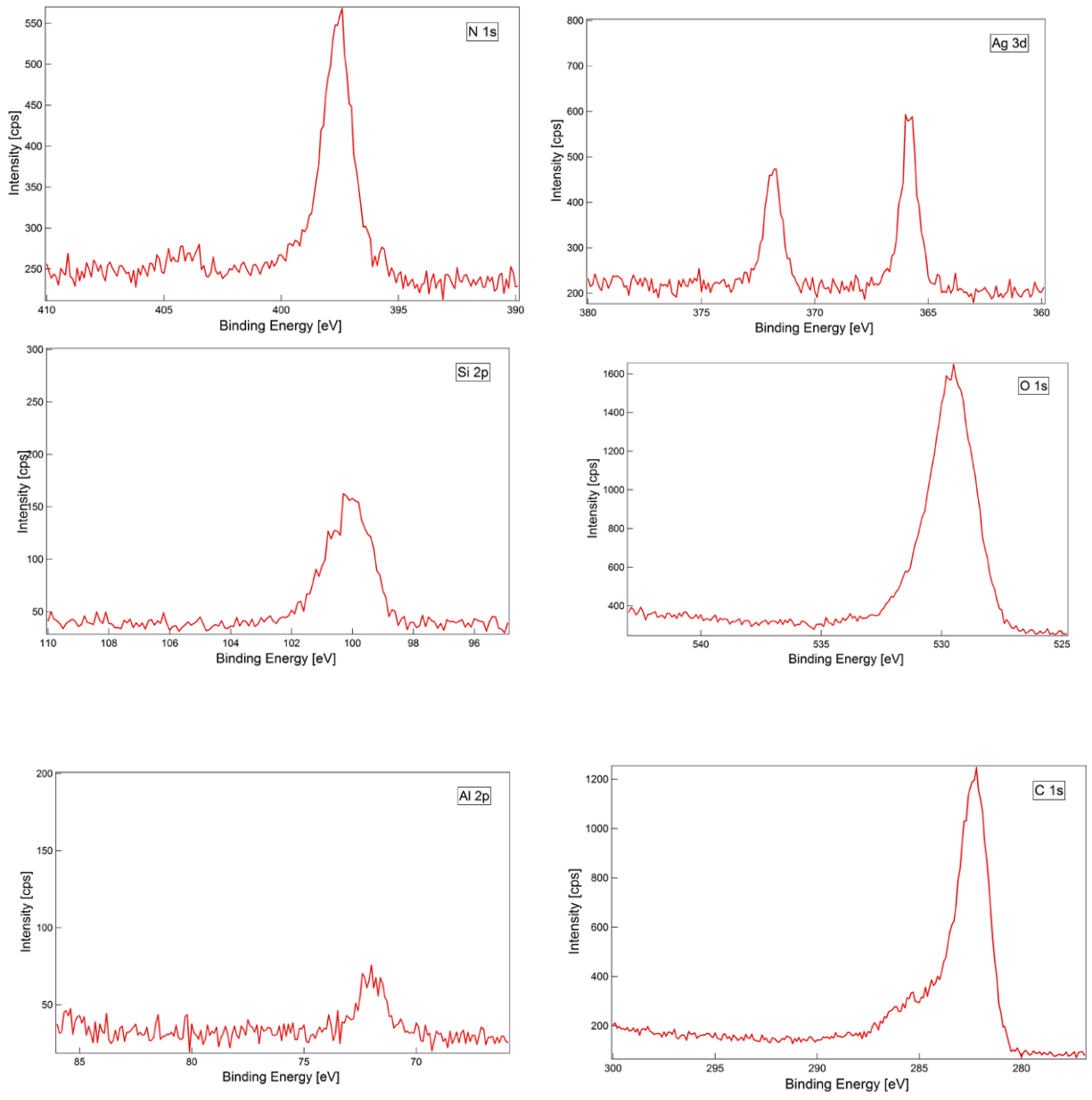

Figure 4: XPS Spectra of Ag/PPY/MMT. The XPS peaks obtained for N 1s, Ag 3d, Si2p, O 1s, Al 2p and C 1s are shown.

Wavenumber/cm^{-1}	Assignment	Originated from
1640	H-O-H bending	Adsorbed water
~3400	hydrogen bonded O–H stretching (water) Broad	Adsorbed water
3622	O-H Stretching (water or MMT)	Water/Montmorillonite
3226	H bonded N-H stretching (PPY)	Polypyrrole
830	Al-Mg-OH deformation	Montmorillonite
877	Al-Fe-OH deformation	
915	Al-Al-OH deformation	
1030	Si–O planar stretching	
1114	Si–O stretching	
1547	- (2,5-substituted pyrrole)	Polypyrrole
1452	Typical polypyrrole ring vibrations.	
1312	=C–H band in plane vibration	
1040	=C–H band in plane vibration.	
1178	N–C stretching band	
889	=C–H out of plane vibration indicating polymerization of Pyrrole	

Table 3: FT-IT Band assignments of montmorrilonite and polypyrrole in the Ag/PPY/MMT composite.

Material	C	O	N	Pd	Ag	Si	Al	Fe	Cr
Ag(I)/ppy	76.68	15.72	7.23	0.00	0.38	0.00	0.00	0.00	0.00
Ag /ppy/MMT	59.75	26.53	7.07	0.00	0.66	4.64	1.35	0.00	0.00

Table 4: Percentage composition of elements as determined by XPS for Ag(I)/PPY and Ag/PPY/MMT composites.

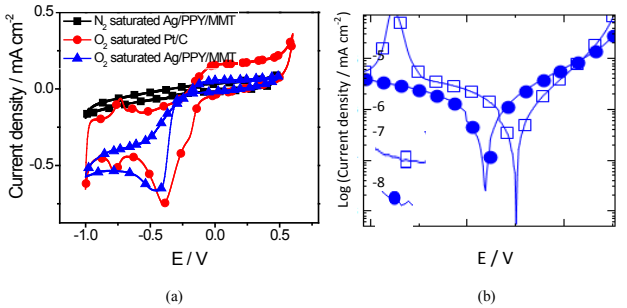

(a) (b)

Figure 5: (a) Cyclic voltammogrammes of Ag/PPY/MMT and C/Pt in N_2-purged and O_2 saturated KOH electrolyte. **(b)** The corresponding Tafel plots for Pt/C and Ag/PPY/MMT electrodes at the scan rate of mV s^{-1}.

treatment followed by H_2O_2 treatment have taken away all the surface Fe(III) species which were present due to isomorphic substitution for Si to give net negative charge for the clay layers. However, bulk Fe(III) in the interior of the clay platelets are not removed. As such although XPS does not detect Fe since there are no Fe(III) in the 2 nm depth from the surfaces of the composite. However, there are Fe(III) in the interior for XRF to detect them. Both XRF and XPS detect the presence of Ag where XRF detects Si: Ag atomic ratio to be 2.72:1 (Table 2) whereas XPS detects that to be 7:1 (Table 4). This shows that most of the silver atoms in the Ag/PPY/MMT composite are present within the interlayer spaces well away from the 2 nm depth from the surfaces. Those at the edges of the interlayer spaces are detected by the XPS.

Oxygen reduction studies

The Ag/PPY/MMT catalyst was mixed with Nafion solution and pasted on a glassy carbon electrode and the cyclic voltammogrammes (CVs) were run in 0.10 M KOH solution as described in the experimental section. The CVs for the N_2-purged system and O_2-staurated system are shown in Figure 5a. The CV of C/Pt 20%w:w is also given in the same figure. The CV of the N_2-purged system just resembles that of typical PPY electronically conducting polymer. However, when the electrolyte is saturated with oxygen gas the oxygen reduction is clearly observed in the negative values of the applied voltage with respect to the saturated calomel electrode. As such, our Ag/PPY/MMT catalyst acts as a good catalyst for the ORHR that is utilized in fuel cells. In order to confirm this we have repeated the experiments with both N_2-purged and O_2-saturated KOH solutions with just the bare glassy carbon electrode as the working electrode and keeping all the other parameters essentially the same as those used in CV experiments done with Ag/PPY/MMT working electrodes. These CVs are featureless and oxygen reduction is not observed even in the O_2-saturated electrolyte. In order to compare the electro-catalytic efficiency of Ag/PPY/MMT with that of Pt/C 20% w/w same experiments were carried out with the latter also. The CV of C/Pt in KOH shows somewhat similar features to that of the composite for same mass loading of the catalytic. This confirms that Ag/PPY/MMT to be a good electrocatalyst for the ORR that is taking place in alkaline fuel cells. Exchange current densities taken from Tafel analysis for Pt/C and Ag/PPy/MMT are 3.09 μAcm^{-2} and 2.91 μA cm^{-2} (Figure 5b). As such the very low-cost catalyst Ag/PPY/MMT can replace expensive C/Pt catalysts used in fuel cells.

Conclusion

In this paper, we have demonstrated that novel and extremely low cost Ag/PPY/MMT catalyst for the oxygen reduction half-reaction of fuel cells functions equally well as traditional and prohibitively expensive C/Pt or C/Pt/Rh catalysts and hence fuel cells could be produced at a very low cost when the novel catalysts are used. The novel catalyst system has been well characterized by several independent methods including XRD, FT-IR, XRF, XPS and so on. Its catalytic ability towards oxygen reduction in an alkaline medium has been compared with the same mass of C/Pt traditional catalyst and found to be very close to that of the expensive latter catalyst. As such, fuel cell powered greener motor vehicles could be realized at an affordable cost to many customers.

References

1. http://www.mlive.com/auto/index.ssf/2015/01/honda_to_debut_hydrogen_fuel_c.html
2. http://www.toyota-global.com/innovation/environmental_technology/fuelcell_vehicle/
3. http://www.cnet.com/news/ford-mercedes-benz-and-nissan-target-2017-for-fuel-cell-vehicles/
4. Markovic NM (2003) Handbook of Fuel Cells-Fundamentals, Technology and Applications. (2ndedn), John Wiley and Sons Ltd, New York.
5. Hamnett A (2003) Handbook of Fuel Cells Fundamentals, Technology and Applications. John Wiley and Sons Ltd, New York.
6. Chunzhi H, Sanket D, Garth B, Srinivas B (2005) PEM Fuel Cell Catalysts: Cost, Performance, and Durability.The Electrochemical Society Interface.
7. Strasser P, Koh S, Anniyev T, Greeley J, More K, et al. (2010) Lattice-strain control of the activity in dealloyed core-shell fuel cell catalysts. Nature Chemistry 2: 454-460.
8. Toda T, Igarashi H, Uchida H, Watanabe M (1999) Enhancement of the Electroreduction of Oxygen on Pt Alloys with Fe, Ni, and Co. J Electrochem Soc 146: 3750-3756.
9. Scott RJ, Wilson OM, Oh SK, Kenik EA Crooks RM, et al. (2004) Bimetallic Palladium-Gold Dendrimer-Encapsulated Catalysts. J Am Chem Soc 126: 15583-15591.
10. Hernandez J, Solla GJ, Herrero E, Aldaz A, Feliu JM, et al. (2007) Electrochemistry of shape-controlled catalysts: Oxygen reduction reaction on

cubic gold nanoparticles. J Phys Chem C 111: 14078-14083.

11. Zhang J, Sasaki K, Sutter E, Adzic (2007) Stabilization of platinum oxygen-reduction electrocatalysts using gold clusters. Science 315: 220-222.
12. Wang C, Daimon H, Onodera T, Koda T, Sun SH, et al. (2008) A General Approach to the Size and Shape Controlled Synthesis of Platinum Nanoparticles and Their Catalytic Reduction of Oxygen. Angew Chem., Int Ed 47: 3588-3591.
13. Wang JX, Inada H, Wu LJ, Zhu YM, Choi YM, et al. (2009) Oxygen reduction on well-defined core-shell nanocatalysts: Particle size, facet, and Pt shell thickness effects. J Am Chem Soc 131: 17298-17302.
14. Ataee EH, Wang L, Nemoto Y, Yamauchi Y (2010) Synthesis of Bimetallic Au@Pt Nanoparticles with Au Core and Nanostructured Pt Shell toward Highly Active Electrocatalysts. Chem. Mater 22: 6310-6318.
15. Li WZ, Chen ZW, Xu LB, Yan YS (2010) Enhanced electrocatalytic activity and durability of Pt particles supported on ordered mesoporous carbon spheres. J. Power Sources 195: 2534-2540.
16. Mazumder V, Chi MF, More KL, Sun SH (2010) Synthesis and Characterization of Multimetallic Pd/Au and Pd/Au/FePt Core/Shell Nanoparticles. Angew Chem., Int Ed 49: 9368-9372.
17. Sun SH, Murray CB, Weller D, Folks L, Moser A, et al. (2000) Monodisperse fept nanoparticles and ferromagnetic fept nanocrystal superlattices. Science 287: 1989-1992.
18. Ahrenstorf K, Heller H, Kornowski A, Broekaert JC, Weller H, et al. (2008) Nucleation and Growth Mechanism of Ni_xPt_{1-x} Nanoparticles. Adv. Funct. Mater 18: 3850-3856.
19. Wang C, Chi MF, Wang GF, Vander VD, Li DG (2011) Correlation Between Surface Chemistry and Electrocatalytic Properties of Monodisperse Pt_xNi_{1-x} Nanoparticles. Adv Funct Mater 21: 147-152.
20. Rajapaksae RMG, Kenji M, Bandara HMN, Rajapakse RMMY, Velauthamurti K, et al. (2010) Preparation and characterization of electronically conducting polypyrrole-montmorillonite nanocomposite and its potential application as a cathode material for oxygen reduction. Electrochimica Acta 55: 2490-2497.
21. Ashton AQ (2011) Advances in research and application.